On the Genesis and Fate of Large Coherent Vortical Structures in Turbulent Shallow Wake Flows

C.F. v.Carmer, V. Weitbrecht & G.H. Jirka
Institute for Hydromechanics, University of Karlsruhe, 76128 Karlsruhe, Germany
carmer@ifh.uni-karlsruhe.de, weitbrecht@ifh.uni-karlsruhe.de, jirka@uni-karlsruhe.de

Abstract: In order to examine the behavior of large-scale eddy structures in shallow turbulent shear flow, a large and well equipped shallow water test facility has been constructed at the Institute for Hydromechanics, University of Karlsruhe. In this 5.5 m wide and 13.5 m long basin - operated at water depths of only a few centimeters - a plane turbulent equilibrium shear flow is produced. In the present study a disturbance is induced to the base flow by forcing it to flow around a single cylindrical body with a diameter D, which is clearly larger than the water depth h. For each flow condition a PIV measuring technique using particles floating at the free surface was employed to obtain horizontal velocity fields, and an image analysis method using digitized video frames has been used to provide depth-averaged concentration fields. The ensemble-mean and phase-averaged fields of velocity and tracer mass from the PIV and planar concentration measurements reveal the transport capacity of these large-scale structures for momentum and mass.

Introduction

Turbulent shallow flows having a limited vertical extent in a horizontally unbounded domain are ubiquitous in our environment, e.g. wide rivers, lakes, estuaries, shallow coastal waters or the stratified atmosphere. Such base flows, which are sheared vertically at the fixed bottom (also at fluid-fluid interfaces), can be disturbed by large-scale instabilities, for example introduced by islands. Large-scale eddy structures caused by such perturbations dominate the momentum and mass transport in the near-wake region. In such a shallow domain the flow field is recognized to deviate significantly from flow structures in an unbounded ambient. On one hand, purely kinematically, the reduced vertical dimension prevents a 3D decay of large vortical structures by secondary transverse instabilities. On the other hand, from dynamical grounds, bottom friction leads either to a complete suppression of the generation of large structures at the obstacle or to a downstream re-stabilization of the wake flow.

The study of wake flows behind cylindrical bodies in shallow turbulent shear flow contributes to the understanding of the genesis and preservation principles of the associated large-scale eddy structures and helps to quantify their transport characteristics for momentum and mass. Different instability mechanisms can be characterized regarding some of their large- and small-scale flow characteristics. A complete representation of the physical phenomena was given by CHEN & JIRKA (1995). A first type of stability ("Vortex Street" - VS) shows a formation which resembles a von Karman vortex street, although here the cylinder Reynolds number Re_D is substantially

larger than in the unbounded case. It is characterized by the alternate separation of large vortical structures directly from the cylinder shoulders which are then advected downstream and decay due to the continous influence of bottom shear. If, compared to the ambient flow conditions in the VS case, the stabilizing effect of bottom friction increases or the destabilizing transverse shear is reduced, the convectively unstable VS wake flow undergoes transition: an absolutely unstable recirculating region ("Unsteady Bubble" - UB) developes behind the obstacle, alternately large eddies shed from the downstream edge of the bubble and advect downstream until they disintregrate and the flow stabilizes. If the forcing due to transverse shear is even weaker, then genaration of large-scale vortices at the end of the recirculation zone is completely suppressed ("Steady Bubble" - SB). Nevertheless, the plane "mixing layers" forming the sides of the steady bubble nourish intermitant vortical structures, but they will disintegrate before they mature to the size of the mixing layer.

Experimental Set-Up and Measuring Techniques

For the analysis of the flow characteristics in such shallow shear flow two primary techniques are used. First, the test facility is supplied with an improved combined Laser-Doppler Velocimetry and Laser Induced Fluorescence (LDV-LIF) technique, which allows for spacially well defined and temporally highly resolved synaptic data of velocity and mass fluctuations. Concerning the turbulence spectra in shallow cylinder wakes, details and results using LDV-LIF are reported in CARMER (2000) and CARMER & JIRKA (2001). Second, we employ a Particle Image Velocimetry (PIV) measuring system and an image analysis technique to gather horizontal velocity and tracer mass distributions. If we focus our interest on the development of quasi 2-D large-scale eddies, whose chacteristic length and time scales are much larger than those of plane shear flow, then we need data with less temporal resolution, but spatially well resolved in a wide area of observation.

For the planar velocity measurements, a PIV system (LaVision) was employed to obtain and process video frames provided by a 12 bit, 1024 x 1280 pixel digital camera (PCO-SensiCam) with a frequency of 7 Hz. Using a 14 mm Nikon lense, undistorted pictures of the horizontal flow field in a 1.2 m wide and 1.4 m long area were captured. As tracer particles floating polypropylene beads (diameter 3 mm) were evenly distributed over the uniform flow upstream of the cylindrical obstacle and advected through the area of observation at the free surface. Because the flow velocities were slow and the floating particles defined the measurement plane of the PIV, we could omit using a laser-generated light-sheet. Typically, the PIV provided horizontal velocity fields on a regular 80 x 64 grid (spacing about 18 mm) with 7 Hz. Detailed information about the PIV system is given e.g. by WEITBRECHT & JIRKA (2001).

Depth-averaged scalar fields were obtained for the same flow configuration as the velocity fields, but not simultaneously, when food coloring was injected as a single point-source at the upstream cylinder perimeter. Video images of the flow were taken in an area of 1.2 m x 1.6 m with 25 Hz and later digitized with a resolution of 3 x 8 bit and 768 x 576 pixels. Dye concentrations were calibrated with a set of background images recorded for identical flow depth and illumination. During the conversion of the gray-scale intensity images to concentration, a space averaging (binning) was applied, finally resulting in scalar fields on a 170 x 128 grid (spacing 9.5 mm) with an effective concentration depth of about 6 bit.

Experiments were conducted for different flow regimes to span the different types of instability and their transition. Here we will present one series of measurements for a vortex street like cylinder wake with the following flow conditions: diameter of circular cylinder D = 63 mm, flow depth h = 38 mm, ambient velocity U_a = 0.143 m/s, bottom friction coefficient c_f = 0.0067. Reynolds numbers based on depth and diameter are Re_h = 5,400 and Re_D = 9,000. The flow is characterized by large eddies alternately separating from the left and right side of the cylinder.

Post Processing Techniques

Since for this investigation the interest is also on the downstream evolution of large coherent vortical structures (LCS), these quasi 2-D vortices have to be identified and to be characterized in the longitudinal development of typical properties. In addition, although no coincidentally sampled velocity and mass data is available from the planar measurements, we also want to study the mass transport capacity of the LCS. Therefore, the data has to be post-processed to provide sets of phase-averaged vector and scalar fields. The general procedure of phase-averaging implies the following steps. At first, the individual periods for each shedding cycle are determined for the velocity fields as well as for the concentration fields. Next, based on the individual cycle periods, the time histories of the vector and scalar fields are re-organized by assigning each field for every timestep to its appropriate phase angle φ. The phase time is then split into a number of phase intervals, and all fields belonging to a certain phase interval are then averaged, which leads to phase-averaged fields for discrete phase angles. Finally, after adjusting the phase lag, both phase-averaged fields are cross-correlated. Using phase-averaged instead of ensemble-averaged data, means to adopt a triple decomposition into mean, periodic and random parts, eg. $u_i = U_i + u'_{p,i} + u'_{r,i}$, instead of a classical Reynolds decomposition into mean and fluctuating parts.

For the identification of a single vortex we check for coherency over the spacial extent of the flow. Following MCWILLIAMS (1984), we make use of the Q values computed from the horizontal velocity fields. The Q function is defined as the difference of the squared strain terms and vorticity term by

$$Q = \left(\frac{\partial u}{\partial x} - \frac{\partial v}{\partial y}\right)^2 + \left(\frac{\partial v}{\partial x} + \frac{\partial u}{\partial y}\right)^2 - \left(\frac{\partial v}{\partial x} - \frac{\partial u}{\partial y}\right)^2 \qquad (1)$$

Because the normal stress (first righthand term) is negligibly small compared to the shear stress (second term), the strain reduces to the shear strain and $-Q$ reduces to the second invariant of ∇u. Flow regions where $Q < 0$ are dominated by vorticity; whereas $Q > 0$ indicates strain dominated regions.

Results

Application of the Q evaluation to the phase-averaged velocity fields $\vec{u}(\varphi, \vec{x})$ identifies large-scale flow structures in the shallow wake of the cylinder. Fig. 1 (left) visualizes the vortex shedding process and the downstream evolution of the LCS, which are indicated by connected circular patterns of negative Q (full isolines). These large vortical structures are surrounded by shear dominated regions (dotted isolines), a small negative threshold Q_{LCS} is used to detect the

edges of the LCS (bold lines). Additionally, vectors indicate the reduced velocity field as it deviates from the undisturbed base flow without any obstacle. Further, when we move the reference frame with the speed of the vortex (0.86 U_a) instead, we find that the center of a vortex, defined as a local minimum of Q, coincides with its center of rotation, and that the stagnation points (intersections of streamlines) coincide with the local maxima of Q.

Also, the evaluation of the mass concentration fields exhibits connected circular regions where the tracer mass is accumulated. Using a Taylor hypothesis for the adjustment of the surface velocity to depth-averaged values, we are able to cross-correlate the velocity and mass fields, which evidences the fact that the regions of high concentration and the vorticity-dominated regions coincide. Fig. 1 (right) illustrates the mass transport within the wake flow for a certain phase angle, displaying color-coded isolines of the concentration $c(\varphi,\vec{x})$ and displaying bold black lines for a small negative Q_{LCS} value used to identify the LCS. Note that here dye was injected continously from a single point source at the upper left shoulder of the cylinder.

Similar to unbounded wake flows a 1-D transport model for momentum and mass can be developed to describe the ensemble mean velocity and scalar fields $\langle \vec{u}(\vec{x}) \rangle$ and $\langle c(\vec{x}) \rangle$ in shallow wake flows. In the following we propose some scaling and functional dependencies, which will also account for the additional influence of bottom shear and vertical confinement, and lead to a closed set of equations for the axial velocity $\langle u(x,y) \rangle$. We will restrict this to wake flows with pronounced vortex-street like instability.

By scaling the velocity defect $U_a - U(x,y)$ with its centerline value $U_a - U_c(x)$ we get a self-similar transverse distribution of the unified velocity defect

$$\frac{U_a - U}{U_a - U_c} = e^{\left(-\alpha \xi^2\right)} \tag{2}$$

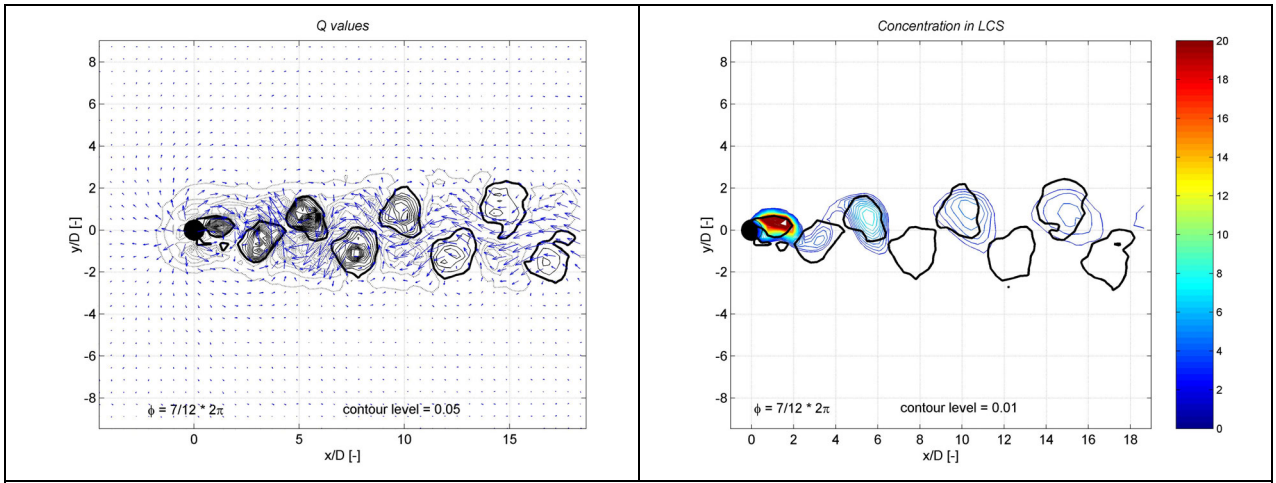

Fig. 1**:** Example for phase-correlated flow field in shallow cylinder wake (D = 63 mm, h = 38 mm, Re_h = 5,400)
left: vectorfield of reduced horizontal velocity, contours are isolines of Q with full lines for vorticity-dominated regions, dotted lines for strain-dominated regions, bold full lines for threshold of Q_{LCS} for LCS identification;
right: continous dye injection at upper left shoulder of cylinder, color-coded contours for mass concetration, superimposed Q_{LCS}

where $\alpha = ln(2)$, U_a is the ambient velocity, $U_c(x) = U(x,0)$ is the centerline velocity, $\xi = y/\delta_u$ is the scaled transverse coordinate, and $\delta_u(x)$ is the wake half-width given by $U_a - U(x,\delta_u) = 1/2\left(U_a - U_c(x)\right)$. In this section the angle brackets $\langle\,\rangle$ to indicate ensemble-averaged values are omitted for brevity. For unbounded plane wakes eq. (2), implying the hypothesis of constant eddy viscosity, fits well to experimental data, exhibiting minor deviations near the edges. The shallow wake data plotted in Fig. 2 confirms eq. (2) also close to the cylinder for velocity defects up to 1/4 U_a.

The self-similar unified velocity defect eq. (2) includes two independent variables, which themselves alter with axial distance. For unbounded wake flows, the centerline wake defect decays with x to the -1/2 power, whereas the wake half-width increases to the power of 1/2. In shallow wakes we could incorporate the damping effect of bottom friction with an exponential function using a friction length scale. We suggest the following proportionalities for the centerline defect velocity (cf. Fig. 3)

$$\frac{U_a - U_c(x)}{U_a} \propto \left(\frac{x}{\delta_{u0}}\right)^{-1/2} e^{-c_f \frac{x}{h}} \tag{3}$$

and for the wake half-width

$$\frac{\delta_u}{\delta_{u0}} \propto \left(\frac{x}{\delta_{u0}}\right)^{1/2} e^{-c_f \frac{x}{h}} \tag{4}$$

where δ_{u0} is an initial measure of the half-width ($\delta_{u0} = \min(\delta_u)$, estimated e.g. with $D/2$) and c_f a mean bottom friction coefficient defined by $\tau_0 = c_f \rho U^2/2$.

Besides the mean features of the shallow wake flow our interest focusses on the LCS, which are essential to this type of flow. Also a whole variety of large scale turbulence properties can be computed from the phase-averaged velocity and scalar fields. Fig. 4 illustrates this with some cross-sectional scalar fluxes resulting from the cross-correlated fields. Triple decomposition of u_i and c yields the mean scalar flux in the i direction

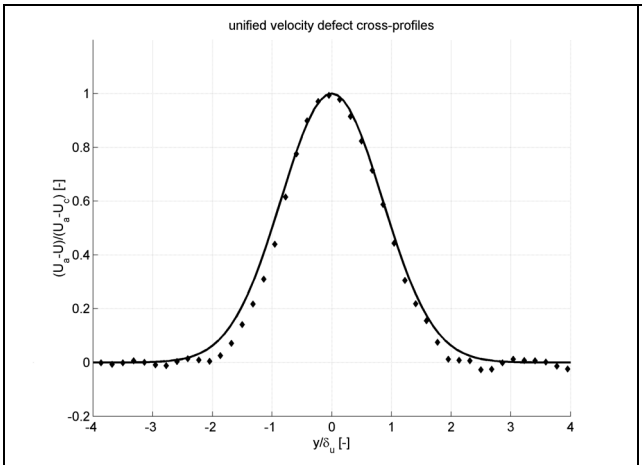

Fig. 2: self-similar transverse distribution of unified velocity defect, black diamonds: measured transverse profiles averaged over $8 < x/D < 32$; full line: eq. (2)

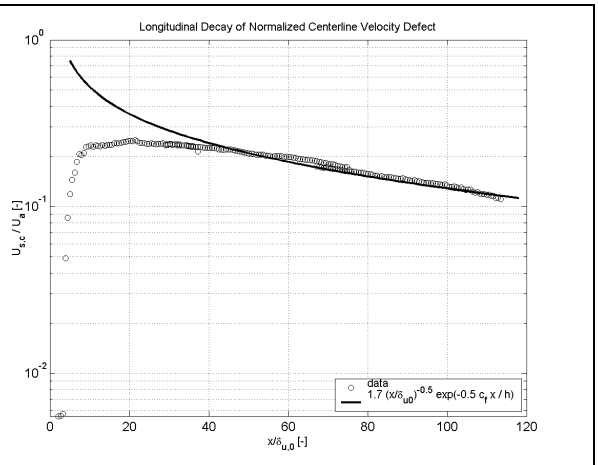

Fig. 3: axial decay of normalized centerline velocity defect, circles: measured data for $x/D \geq 1$; full line: fit with eq. (3)

$$cu_i = CU_i + c'_p u'_{i,p} + c'_r u'_{i,r} + c'_r u'_{i,p} + c'_p u'_{i,r} \quad (5)$$

where the first three right-hand terms are the mean advective, large-scale periodic and small-scale turbulent parts, respectively. Both cross-correlated fluctuating parts will vanish since the fluctuations are decorrelated in this type of wake instability. The small-scale turbulent fluxes are not accessible through this PIV technique, because velocity and concentration measurements are not conducted simultaneously. However, from combined LDV-LIF measurements we know, that the small-scale turbulent axial mass transport rate is two orders of magnitude smaller than the large-scale one and can therefore be neglected. In Fig. 4 the complete longitudinal scalar flux cu (symbol: o) indicates mass conservation and verifies the data acquisition and analysis. The large-scale fluctuating transverse flux $c'_p v'_p$ shows the effective transverse mass transport in total (symbol: +) and due to the LCS (symbol: ◊). Spreading is essentially to the left (away from the wake centerline), the initially very high rate decreases fast until the transverse transport nearly stops.

Summary

Planar measuring techniques for horizontal velocity and concentration fields have been adepted to shallow wake flows. Post-processing procedures to identify large-scale coherent vortical structures using their Q values and to evaluate their transport capacity for momentum and scalar properties from phase-averaged data have been developed. The effect of bottom friction in unstable shear flow has been applied to a shallow cylinder wake to improve the existing model for unbounded wakes. Further analysis will cover the different instability types of shallow wakes to elucidate the various mechanisms of flow stabilization beyond the vortex street like wake.

Acknowledgements

The support of the German Research Council (DFG grants Ji 18/4-1 and Ji 18/8-1) is acknowledged. CFvC would like to thank the colleagues of Dept. of Fluidmechanics at TU Delft for their hospitallity and support during his stay in the Netherlands.

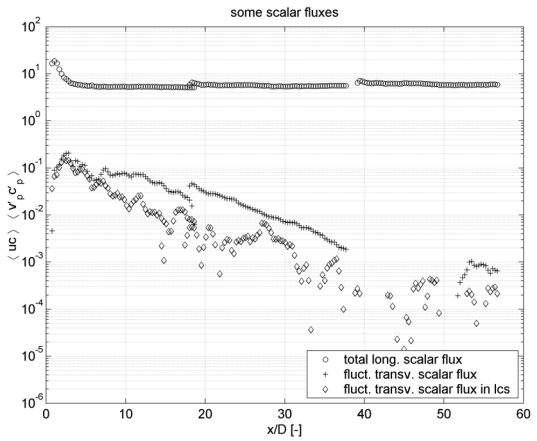

Fig. 4: cross-sectional integrated scalar fluxes, o: total axial mass flux cu; +: large-scale fluctuating transverse mass flux $c'_p v'_p$ along full cross-section; o: only in LCS

References

CARMER, C.F.V. (2000): LDA-LIF System zur Untersuchung großräumiger kohärenter Strukturen in flacher turbulenter Strömung. Delgado, A. et al. (Hrsg., 2000): Lasermethoden in der Strömungsmesstechnik. 8. GALA-Fachtagung. Shaker Verlag, Aachen.

CARMER, C.F.V. & JIRKA, G.H. (2001): On Turbulence and Transport in Shallow Wake Flows. Proceedings 29th IAHR Congress, Beijing, China.

CHEN, D. & JIRKA, G.H. (1995): Experimental study of plane turbulent wakes in a shallow water layer. Fluid Dyn. Res., 16:11-41.

MCWILLIAMS, J.C. (1984): The emergence of isolated coherent vortices in turbulent flow. J. Fluid Mech., 146:21-43.

WEITBRECHT, V. & JIRKA, G.H. (2001): Flow Patterns and Exchange Processes in dead zones of Rivers. Proceedings 29th IAHR Congress, Beijing, China.